Hindawi
International Journal of Antennas and Propagation
Volume 2018, Article ID 9409152, 9 pages
https://doi.org/10.1155/2018/9409152

Research Article

UHF Metamaterial Absorber with Small-Size Unit Cell by Combining Fractal and Coupling Lines

Shicheng Fan and Yaoliang Song

Department of Electronic Engineering, Nanjing University of Science and Technology, Nanjing 210094, China

Correspondence should be addressed to Yaoliang Song; ylsong@njust.edu.cn

Received 13 March 2018; Revised 3 June 2018; Accepted 12 July 2018; Published 18 September 2018

Academic Editor: Giuseppe Castaldi

We present a perfect UHF metamaterial absorber by combining coupling lines and fractal lines with a very small unit cell. The proposed absorber consists of a surface metal structure and metallic background plane, separated by a dielectric substrate and air. Simulation results show that the absorber has an absorption peak at 442 MHz with 99.73% absorptivity. The ratio between a lattice constant and resonance wavelength is 1/68, significantly less than the existing absorber. The design principle is introduced in detail according to the absorption mechanism of the proposed absorber. Moreover, the absorption peaks remain high with large angles of incidence for both TE and TM polarizations. Due to the small ratio, it can be widely used in radiation suppression for microwave relay communication such as mobile communication and wireless network by changing the parameters of the structure.

1. Introduction

Perfect metamaterial absorbers were first proposed by Landy et al. in 2008 [1], and these had broad application prospects in the fields of radar target stealth, antenna design, and electromagnetic protection [2–5]. The incident electromagnetic wave can be absorbed almost 100 percent by the rational design unit cell and dielectric materials. To date, much work has been made on absorbers to achieve multiband absorption and broadband absorption due to its important applications in microwave, terahertz, and optical frequency [6–15]. A dual-band polarization-independent metamaterial absorber has been designed using a fractal square loop. Dual-band and triple-band polarization-independent metamaterial absorbers have been designed by making arrays of different structures [16]. A flexible ELC resonator is designed, and by scaling the ELC resonator, single-band, dual-band, and triple-band absorbers can be obtained easily. Most of the absorber designs are focused on the S, C, and X bands of microwave or higher frequency bands because the metamaterial absorber requires a large number of periodic structures. However, the lattice constant of the existing absorbers is not small enough, typically only 1/3–1/5 of the wavelength. Although the absorption peaks of the absorber can be extended to any frequencies by changing the size, the absorbers have a large-size unit cell for some applications at UHF band such as 315 MHz, 433 MHz, and 2.4 GHz.

A large number of efforts have been made on absorbers to achieve an UHF band. In [17], the snake-shape design was employed to realize the thin and small-size unit cell and the frequency of the resonance peak is determined by controlling the length of snake bar. Reference [18] also has a design method based on the corrugated surface to realize low frequency. By inserting the periodic square-pillar array into the required resonant structure, it is easy to realize the control of resonance frequency. The resonant frequency can also be reduced by using an intermediate dielectric layer with a high dielectric constant [19]. In this paper, an UHF metamaterial absorber has been proposed. A fractal can be infinitely long on a finite area. Based on the fractal and coupling principle, we greatly reduce the ratio between unit cell size and wavelength by designing the top-patterned copper. The proposed absorber also possesses many advantages, such as being polarization insensitive and wide angled and

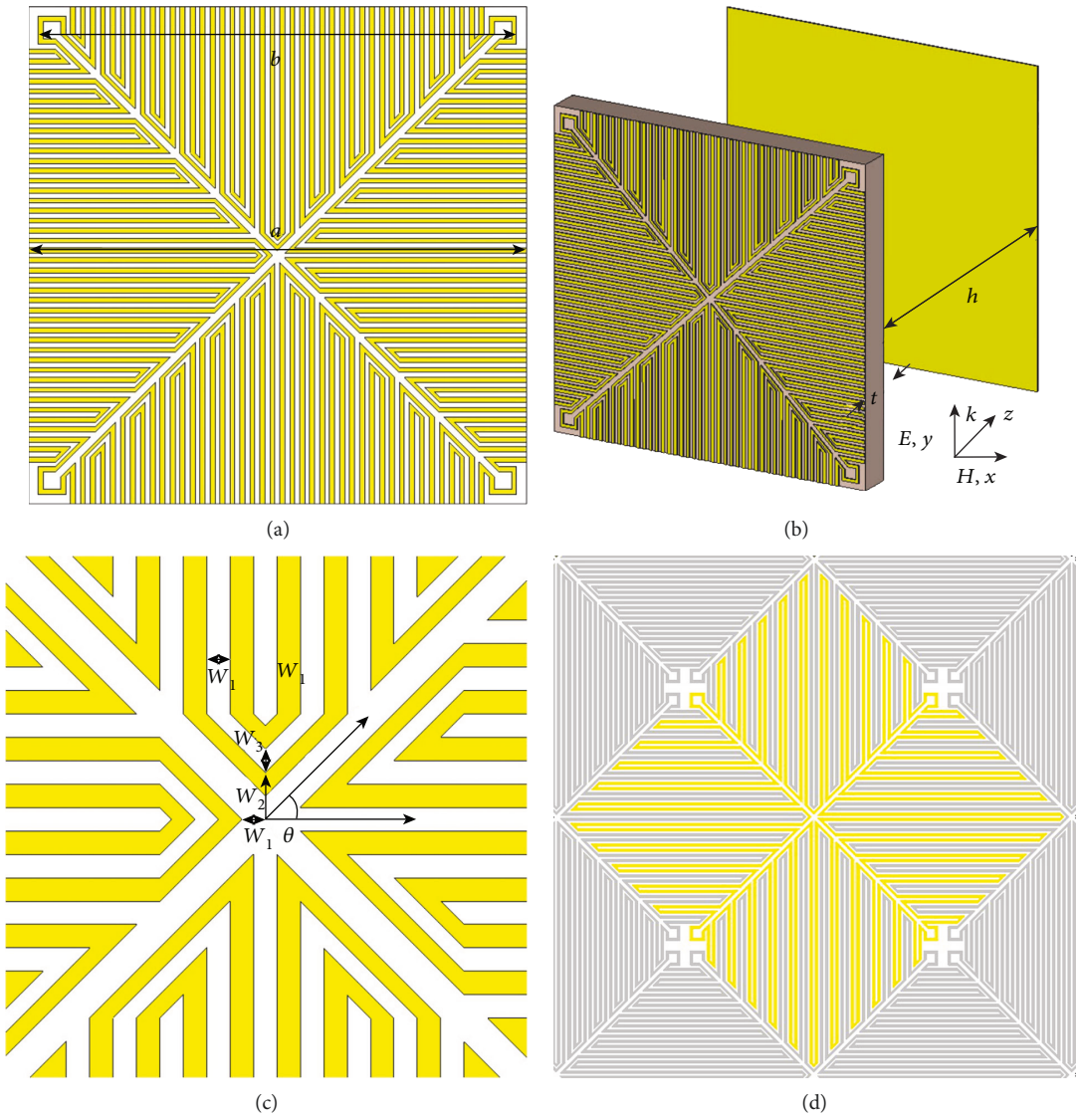

Figure 1: (a) The front view of the proposed absorber; (b) perspective view of the proposed absorber; (c) enlarged view of the top layer; and (d) complete unit cell surface structure.

having a low profile and variable frequency. Moreover, we discuss the principle and design process to add a new way in the area of UHF band absorber with a small size.

2. Design and Simulations

The proposed absorber is designed by combining coupling lines and fractal lines. The surface-patterned copper is a closed curve made of twisted copper wire which not only is a part of the fractal line but also is a part of the coupling line. The top view of the unit cell geometry of the proposed absorber is shown in Figure 1(a). Both the top-patterned copper and bottom ground plate are 0.035 mm thick with an electric conductivity of 5.8×10^7 S/m. The Teflon material is selected for the dielectric substrate, with the relative permittivity of $\varepsilon_r = 2.1$ and the dielectric loss tangent of $\tan \delta = 0.0002$. Between the bottom ground plate and the dielectric substrate is a layer of air with a thickness of

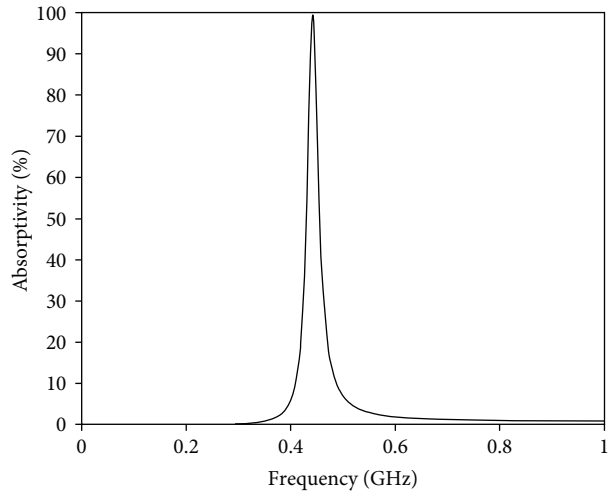

Figure 2: Simulated absorption spectra of the proposed absorber.

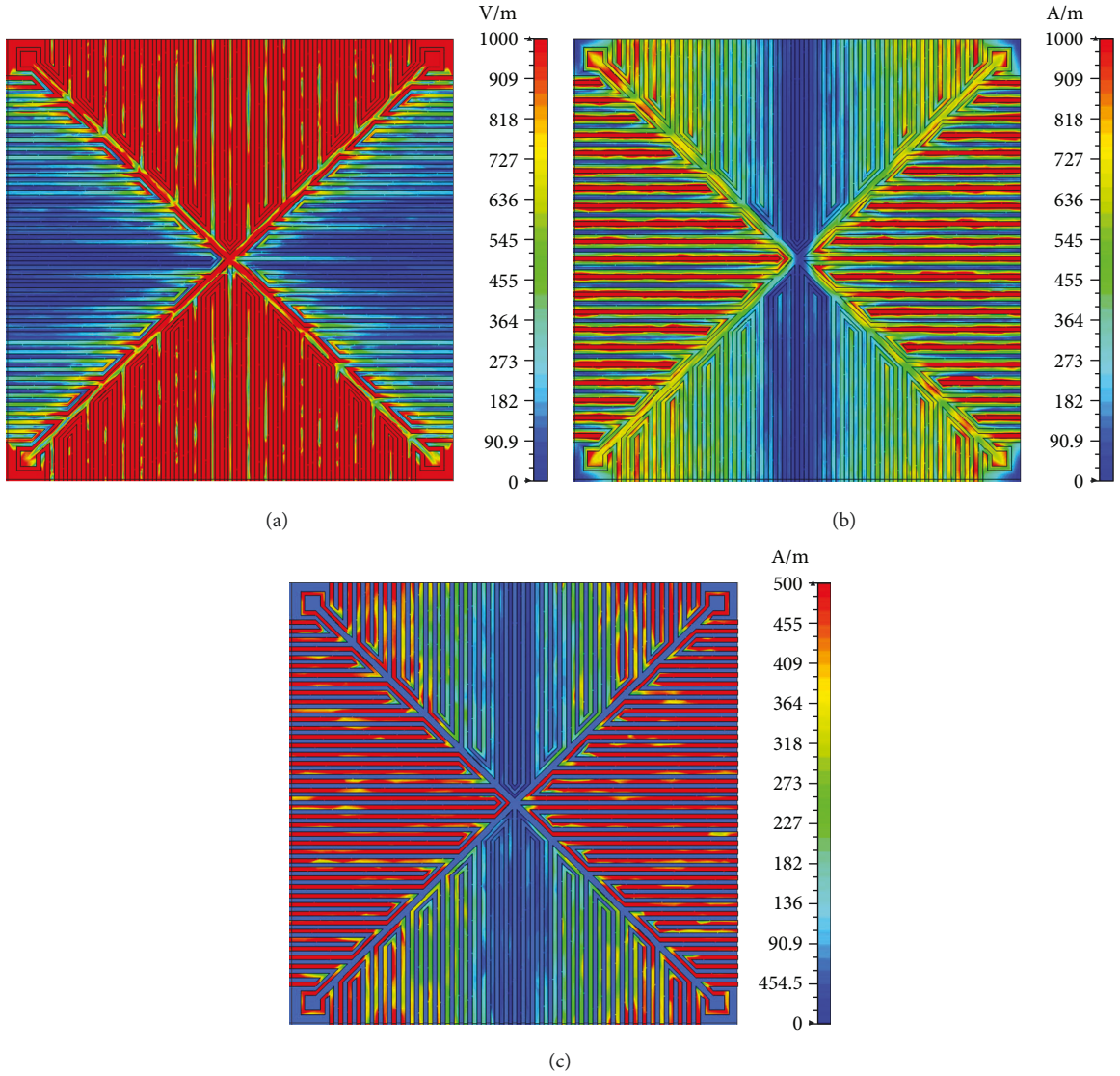

Figure 3: (a) The electric field distributions, (b) magnetic field distributions, and (c) surface current density at 442 MHz.

8.6 mm. The complete structure is actually a square ring with curves as shown in the proposed absorber with a periodic pattern in Figure 1(d). The structure has the following geometrical parameters: $a = 10$ mm, $b = 9.6$ mm, $h = 8.6$ mm, $t = 1$ mm, $b = 9.6$ mm, $W_1 = 0.1$ mm, $W_2 = 0.1$ mm, $W_3 = 0.1$ mm, and $\theta = 45^\circ$. The line width is 0.1 mm.

The unit cell structure is simulated in CST Microwave Studio based on the finite element method. Periodic unit cell boundary conditions were used along the x and y directions. The floquet port is modeled to excite incident waves traveling in the z direction. The absorptivity can be calculated as $A(\omega) = 1 - |S_{11}(\omega)|^2 - |S_{21}(\omega)|^2$, where $S_{11}(\omega)$ and $S_{21}(\omega)$ are the absorption reflection and transmission, respectively. Because of a completely metallic ground plate, $S_{21}(\omega)$ is zero. The simulated result is depicted in Figure 2. From the result, it can be seen that the proposed absorber had an absorption peak at 442 MHz with a peak absorption rate of 99.73%. The absorber's full width half maximum is 5.6% (from 430 MHz to 455 MHz) and it can be applied to wireless security. The use of air is to reduce the weight of the absorber so that it has a wider range of applications. Actually, the air layer can keep a gap of 8.6 mm from the ground with the support of plastic screws. Moreover, in order to understand the physical mechanism of this absorber, the field distributions and surface current are shown in Figure 3. Obviously, the current is mainly along the copper line, due to the twists and turns in the copper line, greatly increasing the length of the current, thereby reducing the resonant frequency of the absorber.

The constitutive electromagnetic parameters can be computed by S_{11} and S_{18}. The constitutive parameters can be retrieved, and the effective permittivity ε and effective permeability μ are calculated and shown in Figure 4. The metamaterial absorber changes its dielectric constant and permeability through structural design. Meanwhile, the real and imaginary parts of the normalized input impedance Z should be 1 and 0 at the frequency of absorption. This implies that ε and μ values should match at the absorption frequency, as the structure is primarily excited due to the

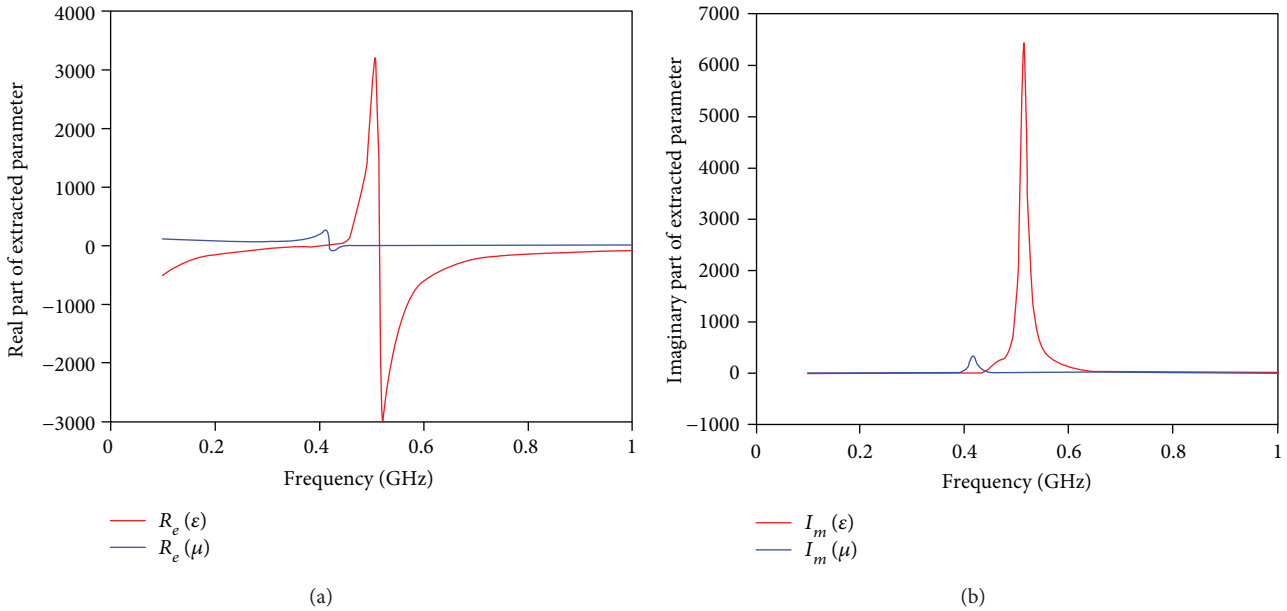

Figure 4: Comparison of extracted constitutive electromagnetic parameters. (a) Real parts and (b) imaginary parts.

electric field. Thus, ε is varying over a large range compared to μ values, both in the real and imaginary parts. Therefore, the absorption mechanism is to match the space impedance by adjusting the electromagnetic parameters, then the current excited by the electric field leads to strong electromagnetic absorptions.

3. Discussion

In order to explore the method of reducing the ratio between the unit size and the incident wavelength, five structures were designed to verify the influence of different types of structures to the resonance frequency. The most basic structure is the square ring as shown in Figure 5(a). The resonant frequency is related to the length of the structure [20]. $f \sim 1/(\sqrt{\varepsilon} * L)$, where ε is the relative permittivity of the dielectric, and L is the length of the closed line. Therefore, the length of the structure is inversely proportional to the resonant frequency. A fractal can be of infinite length on a limited area. Based on this, we designed the second structure as shown in Figure 5(b).

The equivalent circuit of the absorber behaves as a parallel RLC circuit [21]:

$$\begin{aligned} Z_i &= Z_s \| Z_{TML}, \\ Z_s &= R_s + j\omega L_s + \frac{1}{j\omega C_s}, \\ Z_{\mathrm{TML}} &= Z_d + Z_c \\ &= j\sqrt{\frac{(\mu_0\mu_r)}{(\varepsilon_0\varepsilon_r)}}\tan(kd) + R_d + \frac{1}{j\omega C_c}, \end{aligned} \tag{1}$$

where L_s is the absorber inductance corresponding to the length of the square ring and C_s is the structure capacitance between two adjacent unit cells. R_s is the resistance of the top copper line. Z_s is the impedance of the surface structure. Z_{TML} is the substrate impedance. ε_r and μ_r are the electric permittivity and magnetic permeability of the dielectric substrate, respectively. $k = k_0\sqrt{\varepsilon_r\mu_r}$ is the wave number of the incident wave in the substrate. R_d is the equivalent resistance due to dielectric loss and C_c is the coupling capacitance due to a periodic structure. The dielectric layer loss is small, so the value of R_d is small. Z_i is the impedance of the absorber. At resonance frequency, the real part of Z_i will match closely with the free space impedance and the imaginary part will tend to infinity. The resonance frequency of the structure is determined by the LC circuit resonance $f = 1/2\pi\sqrt{LC}$, where L and C are inductance and capacitance, respectively. Based on this, reducing the distance between two unit cells will increase the capacitance C_s and C_c. Then, the resonance frequency will decrease by this way. The third structure is designed as shown in Figure 5(c). We increase the number of fractals and make it more closer to increase the coupling between the cells to further reduce the resonance frequency. The fourth structure is shown in Figure 5(d). Due to the actual fabrication, the distance between unit cells is limited and another way is needed to further increase the coupling between the unit cells, such as loading by interdigital capacitors, which is a copper line densely arranged between adjacent unit cells [22]. The fifth structure is designed as shown in Figure 5(e).

All the structures have been simulated in CST Microwave Studio based on the finite element method. Each structure has adjusted to the optimum thickness of the dielectric layer. From the results shown in Figure 6, it can be seen that square ring with a 0.35 mm-thick dielectric layer has an absorption peak at 6.23 GHz with a peak absorption rate of 99.45%. The ratio between the structure size and the wavelength is 1/4.8. The more compact structure with a 0.35 mm-thick dielectric layer has an absorption peak at 5.75 GHz with a

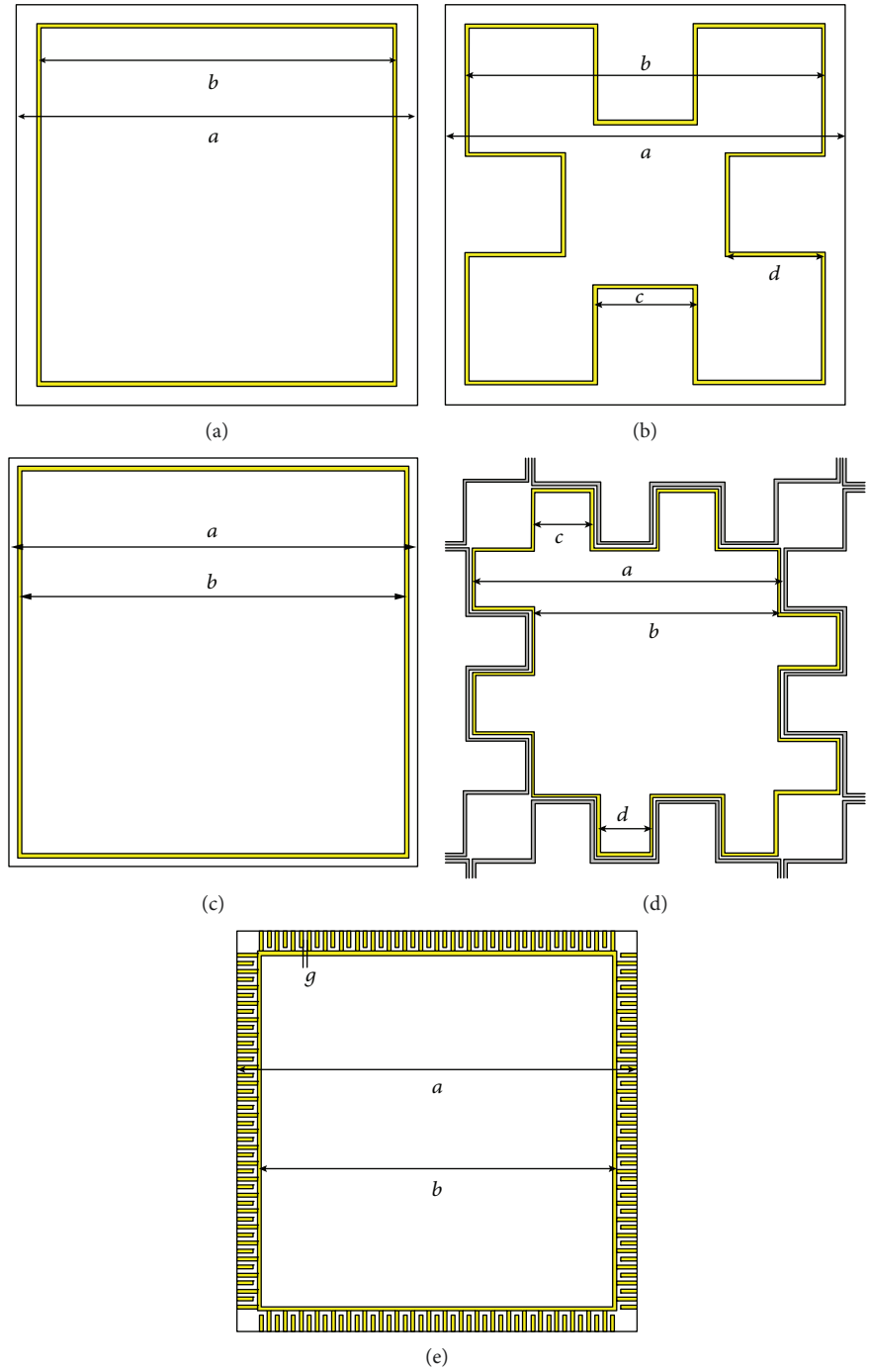

Figure 5: (a) Square ring: $a = 10$ mm and $b = 9$ mm. (b) Fractal: $a = 10$ mm, $b = 9$ mm, $c = 2.6$ mm, and $d = 2.5$ mm. (c) More compact: $a = 9.4$ mm and $b = 9$ mm. (d) Compact fractal: $a = 10$ mm, $b = 8$ mm, $c = 2$ mm, and $d = 1.8$ mm. (e) Loaded interdigital capacitors: $a = 10$ mm, $b = 9$ mm, and $g = 0.1$ mm. The line width for all is 0.1 mm.

peak absorption rate of 98.34%. The ratio between the structure size and the wavelength is 1/5.6. The fractal square ring with a 0.65 mm-thick dielectric layer has an absorption peak at 4.4 GHz with a peak absorption rate of 99.84%. The ratio between the structure size and the wavelength is 1/6.8. The structure-loaded interdigital capacitors with a 0.8 mm-thick dielectric layer has an absorption peak at 2.255 GHz with a peak absorption rate of 96.69%. The ratio between the structure size and the wavelength is 1/13.3. The more compact fractal with a 0.8 mm-thick dielectric layer has an absorption peak at 2.39 GHz with a peak absorption rate of 99.19%. The ratio between the structure size and the wavelength is 1/12.5.

The resonance frequency of the basic structure is decreased in different ways. Comparing Figures 5(a) and 5(b), the resonant frequency can be reduced by increasing

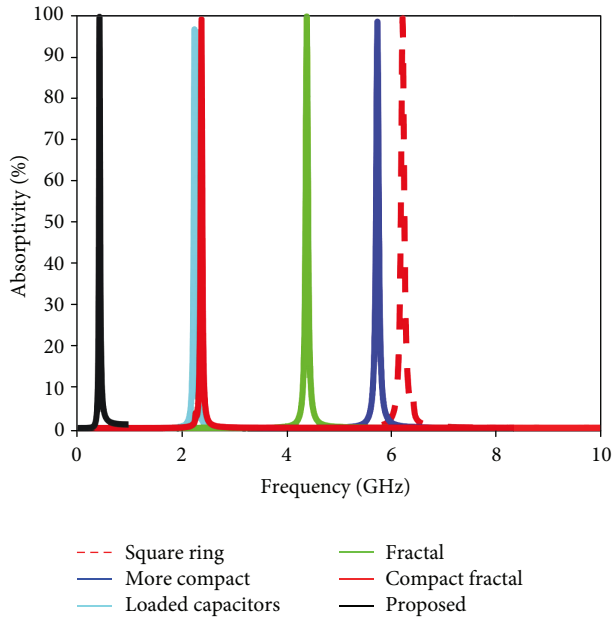

Figure 6: Simulated absorption spectra of the proposed absorber and four basic absorbers.

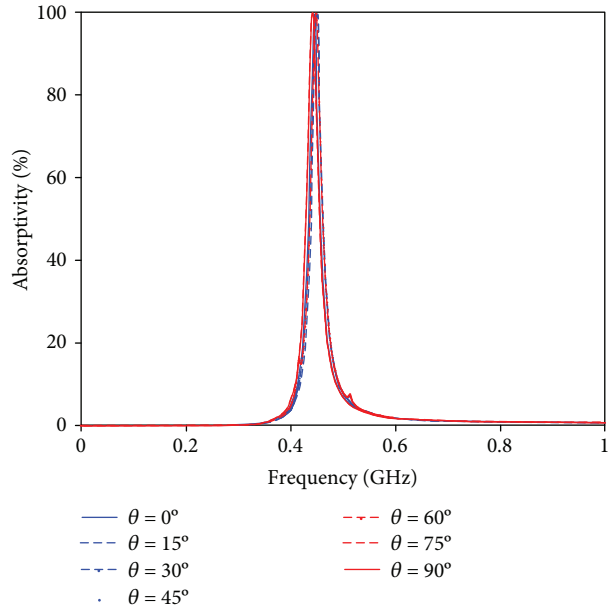

Figure 7: Simulated absorptivity for different polarization angles.

the length by a fractal. Comparing Figures 5(a) and 5(c), the resonant frequency can be reduced by reducing the distance between two unit cells. Comparing Figures 5(a) and 5(e), the resonant frequency can be reduced by loading interdigital capacitors. Combining these three methods, the added interdigital capacitors are part of the fractal; at the same time, the unit cell distance is reduced. The proposed absorber was designed. As a result of the design incorporating all of the above ways, the resonant frequency of the proposed absorber is much smaller than the above structures. Moreover, the resonant frequency can be adjusted by changing the structural parameters such as W_3 which is the distance between structures. The frequency of the resonance peak can also be determined by controlling the number of the coupling line. Like the previous absorbers, the size of the structure still controls the absorption frequency. So it is easy to design an absorber suitable for the UHF bands of 315 M, 433 M, and 2.4 G.

The proposed absorber is not strictly rotationally symmetrical. However, for the long line, the change is very small. As shown in Figure 7, it is clear that the proposed absorber is polarization insensitive at normal incidence. It shows that the absorption rate remains unchanged at different polarization angles (θ) and there is a slight frequency shift of less than 9 MHz for all the peaks. In addition, the absorber is also simulated with different incidence angles (ϕ) under both TE and TM polarizations. For TE polarization, the incident electric field vector is invariant and perpendicular to the incident direction. For TM polarization, the incident magnetic field vector is invariant and perpendicular to the incident direction. Figure 8 shows the results of the proposed absorber. It is observed that the absorptivity remains high with the incident angle up to 60° under TE polarization. The main function is the electric field. Under TE polarization, the electric field direction is unchanged, as the incident electric field decreases and cannot efficiently excite the current, and thus, the absorption rate decreases at 80°. It is observed that the absorptivity remains high with the incident angle up to 40° under TM polarization. When the incident angle is greater than 45°, the incident electric field influences the resonance between the units; the resonant frequency moves meanwhile the absorptivity decreases. The increase in absorption frequency is due to the fact that as the incident angle increases under TM polarization, the equivalent medium thickness increases. $C \sim S/d$, that is, as the thickness d becomes larger, both capacitances C_s and C_c decrease and the resonance frequency increases.

4. Experimental Results

To verify the correctness of the simulated absorption performance, we have fabricated a prototype sample based on the optimized geometric parameters using the laser ablation machine. Due to the limitations of the measuring equipment, the horn antennas, prototype sample, and microwave anechoic chamber cannot be used at 440 MHz. We have fabricated a prototype sample based on 2.4 GHz. The surface is 20×20 unit cells with an 88 mm × 88 mm × 0.1 mm polyimide film prepared as a middle dielectric layer. The air layer can keep a gap of 1.1 mm from the ground with the support of a sponge. The bottom is a layer of copper foil affixed to the rubber shown in Figure 9. The use of an air layer greatly reduces the weight of the entire absorber. In the microwave anechoic chamber, a pair of double-ridge broadband horn antennas (1–18 GHz) connected to a vector network analyzer (PNA-XN5244A) is used to measure the reflectivity of the proposed absorber. To ensure the remote field conditions, the distance between the absorber

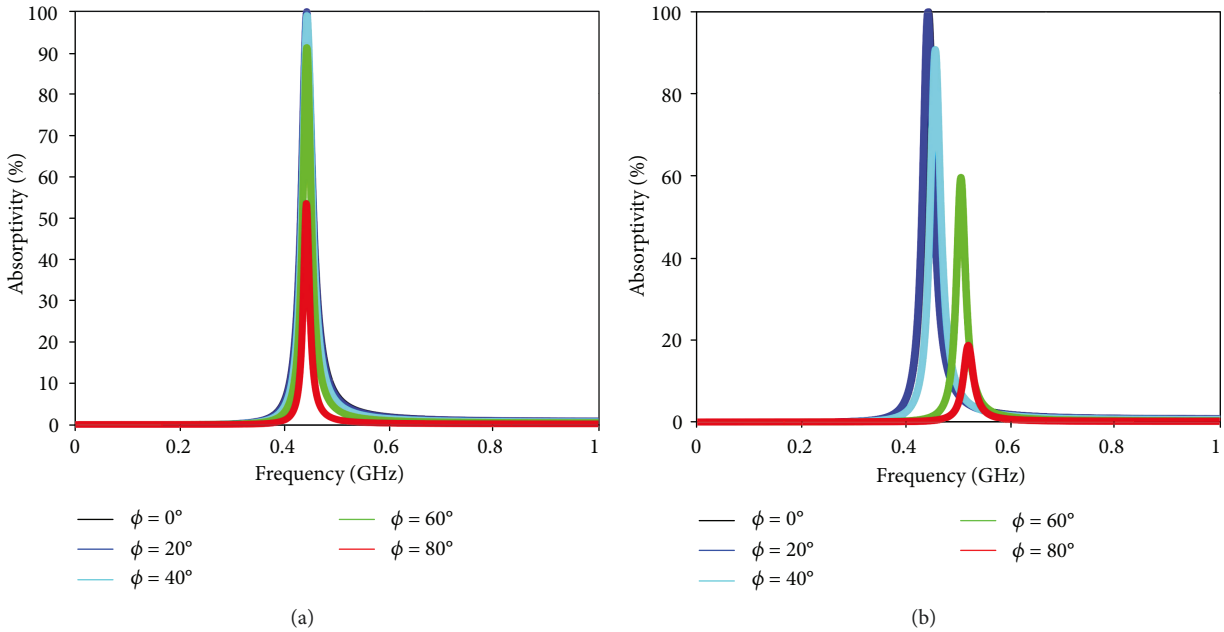

Figure 8: (a) Simulated absorptivity for different incidence angles for TE (a) and TM (b) polarizations.

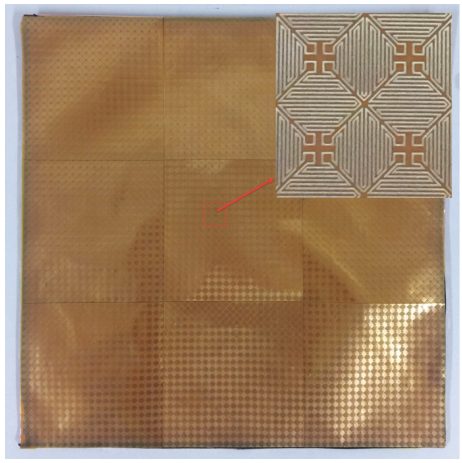

Figure 9: Photography of the fabricated active structure.

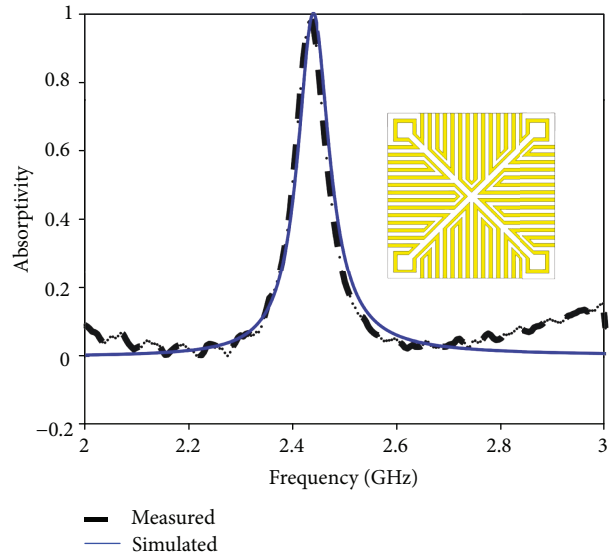

Figure 10: Measured reflection coefficients of the proposed absorber.

and antennas is set as 2 meters. First, the reflection coefficient of the copper foil which has the same size as the proposed absorber is measured. Then, the reflection of the absorber is measured by keeping the sample in the same position. The reflection coefficients measured from the copper surface as well as from the fabricated structure incorporate all the imperfections into the account, like edge reflection, scattering loss, diffraction loss, and so on, and cancels them out during subtraction [4].

As shown in Figure 10, the measured results present an absorption peak at 2.44 GHz which are in good agreement with the simulation. It is noted that the small deviation between measured results and simulation results may be due to fabrication tolerance. This result verifies the practicality of the proposed absorber.

5. Conclusion

In summary, we have proposed a design method by combining fractal lines and coupling lines to realize an UHF absorber. The proposed absorber exhibits an absorption peak at 442 MHz with 99.73% absorptivity. We elaborated on the design principles and processes. Furthermore, absorbers of different frequencies suitable for the UHF band can be designed by changing the structure parameters. The simulated surface current and field distributions are illustrated to better understand the absorption mechanism. Moreover,

Table 1: Comparison of the proposed absorber with the earlier published absorber structures.

Absorber	Operating frequency	Unit cell size	Thickness	Polarization insensitive	Ratio
Reference [17]	403.3 MHz	25.2 mm × 25.2 mm	12 mm	No	1/30
Reference [18]	320 MHz	45 mm × 45 mm	15.2 mm	No	1/21
Reference [19]	1.22 GHz	10.92 mm × 10.92 mm	1 mm	Yes	1/22.5
Proposed	2.4 GHz	4.4 mm × 4.4 mm	1.2 mm	Yes	1/28
Proposed	442 MHz	10 mm × 10 mm	9.6 mm	Yes	1/68

the proposed absorber has many advantages such as being polarization insensitive and wide angled so that it has broader absorber applications. The size of the proposed absorber is much smaller than the existing structure as shown in Table 1. The experimental results coincide well with the simulation results. The smaller structure can be better applied to radiation suppression from mobile and other electronic equipment.

Data Availability

The data used to support the findings of this study are included within the article.

Conflicts of Interest

The authors declare that they have no conflicts of interest.

Acknowledgments

This work was supported by the National Natural Science Foundation of China (nos. 61571229 and 61271331).

References

[1] N. I. Landy, S. Sajuyigbe, J. J. Mock, D. R. Smith, and W. J. Padilla, "Perfect metamaterial absorber," *Physical Review Letters*, vol. 100, no. 20, article 207402, 2008.

[2] M. Li, Z. Yi, Y. Luo, B. Muneer, and Q. Zhu, "A novel integrated switchable absorber and radiator," *IEEE Transactions on Antennas and Propagation*, vol. 64, no. 3, pp. 944–952, 2016.

[3] W. Zhou, P. Wang, N. Wang, W. Jiang, X. Dong, and S. Hu, "Microwave metamaterial absorber based on multiple square ring structures," *AIP Advances*, vol. 5, no. 11, article 117109, 2015.

[4] M. Agarwal, A. K. Behera, and M. K. Meshram, "Wide-angle quad-band polarisation-insensitive metamaterial absorber," *Electronics Letters*, vol. 52, no. 5, pp. 340–342, 2016.

[5] W. Li, X. Y. Cao, J. Gao, Y. Zhao, H. H. Yang, and T. Liu, "Low-RCS waveguide slot array antenna based on a metamaterial absorber," *Acta Physica Sinica*, vol. 64, article 094102, 2015.

[6] S. Shang, S. Yang, L. Tao, L. Yang, and H. Cao, "Ultrathin triple-band polarization-insensitive wide-angle compact metamaterial absorber," *AIP Advances*, vol. 6, no. 7, article 075203, 2016.

[7] J. Hao, R. Niemiec, L. Burgnies, E. Lheurette, and D. Lippens, "Broadband absorption through extended resonance modes in random metamaterials," *Journal of Applied Physics*, vol. 119, no. 19, article 193104, 2016.

[8] R. Yahiaoui and H. H. Ouslimani, "Broadband polarization-independent wide-angle and reconfigurable phase transition hybrid metamaterial absorber," *Journal of Applied Physics*, vol. 122, no. 9, article 093104, 2017.

[9] S. An, H. Xu, Y. Zhang et al., "Design of a polarization-insensitive wideband tunable metamaterial absorber based on split semi-circle ring resonators," *Journal of Applied Physics*, vol. 122, no. 2, article 025113, 2017.

[10] L. Li and Z. Lv, "Ultra-wideband polarization-insensitive and wide-angle thin absorber based on resistive metasurfaces with three resonant modes," *Journal of Applied Physics*, vol. 122, no. 5, article 055104, 2017.

[11] H. Sheokand, S. Ghosh, G. Singh et al., "Transparent broadband metamaterial absorber based on resistive films," *Journal of Applied Physics*, vol. 122, no. 10, article 105105, 2017.

[12] M. Wu, X. Zhao, J. Zhang et al., "A three-dimensional all-metal terahertz metamaterial perfect absorber," *Applied Physics Letters*, vol. 111, no. 5, article 051101, 2017.

[13] C. Zhang, Q. Cheng, J. Yang, J. Zhao, and T. J. Cui, "Broadband metamaterial for optical transparency and microwave absorption," *Applied Physics Letters*, vol. 110, no. 14, article 143511, 2017.

[14] S. Liu, H. Chen, and T. J. Cui, "A broadband terahertz absorber using multi-layer stacked bars," *Applied Physics Letters*, vol. 106, no. 15, article 151601, 2015.

[15] Y. He, J. Jiang, M. Chen, S. Li, L. Miao, and S. Bie, "Design of an adjustable polarization-independent and wideband electromagnetic absorber," *Journal of Applied Physics*, vol. 119, no. 10, article 105103, 2016.

[16] S. Bhattacharyya, S. Ghosh, and K. Vaibhav Srivastava, "Triple band polarization-independent metamaterial absorber with bandwidth enhancement at X-band," *Journal of Applied Physics*, vol. 114, no. 9, article 094514, 2013.

[17] Y. J. Yoo, H. Y. Zheng, Y. J. Kim et al., "Flexible and elastic metamaterial absorber for low frequency, based on small-size unit cell," *Applied Physics Letters*, vol. 105, no. 4, article 041902, 2014.

[18] N. Wang, X. Dong, W. Zhou, C. He, W. Jiang, and S. Hu, "Low-frequency metamaterial absorber with small-size unit cell based on corrugated surface," *AIP Advances*, vol. 6, no. 2, article 025205, 2016.

[19] B. Lin, S. Zhao, X. Da et al., "Triple-band low frequency ultra-compact metamaterial absorber," *Journal of Applied Physics*, vol. 117, no. 18, article 184503, 2015.

[20] Y. Pang, H. Cheng, Y. Zhou, and J. Wang, "Analysis and design of wire-based metamaterial absorbers using equivalent circuit approach," *Journal of Applied Physics*, vol. 113, no. 11, article 114902, 2013.

[21] S. Ghosh and K. V. Srivastava, "2015 index IEEE antennas and wireless propagation letters vol. 14," *IEEE Antennas and Wireless Propagation Letters*, vol. 14, pp. 1827–1880, 2015.

[22] L. Lu, S. B. Qu, X. Su, Y. B. Shang, J. Q. Zhang, and P. Bai, "Simulation and experiment demonstration of an ultra-thin wide-angle planar metamaterial absorber," *Physics*, vol. 62, article 208103, 2013.